Bioorganic & Medicinal Chemistry 18 (2010) 6995–7000

Contents lists available at ScienceDirect

Bioorganic & Medicinal Chemistry

journal homepage: www.elsevier.com/locate/bmc

Gentisides C–K: Nine new neuritogenic compounds from the traditional Chinese medicine *Gentiana rigescens* Franch

Lijuan Gao [a], Lan Xiang [b], Yan Luo [a], Guangfa Wang [a], Jinyou Li [a], Jianhua Qi [a,*]

[a] College of Pharmaceutical Sciences, Zhejiang University, Yu Hang Tang Road 388, Hangzhou 310058, China
[b] College of Biosystems Engineering and Food Science, Zhejiang University, Hangzhou 310029, China

ARTICLE INFO

Article history:
Received 21 June 2010
Revised 7 August 2010
Accepted 10 August 2010
Available online 13 August 2010

Keywords:
Gentisides
Neuritogenic compounds
Gentiana rigescens Franch
PC12 cells
Nerve growth factor

ABSTRACT

Nine new alkyl 2,3-dihydroxybenzoates, gentisides C–K, were isolated from the traditional Chinese medicine *Gentiana rigescens* Franch. Their structures and stereochemistry were elucidated by spectroscopic methods, and comparison of the specific rotation with that of the gentiside B. These metabolites are additional members of the gentisides which belong to a novel class of neuritogenic compounds. They are structurally different from one another because they possess varying alkyl chain lengths, with or without an isobutyl or isopropyl group at the end of the alkyl chain. These compounds are potent inducers of neurite outgrowth on PC12 cells. The gentiside C possessing the shortest alkyl chain length exhibited the highest neuritogenic activity among all of the gentisides. Gentiside C showed a significant neuritogenic activity at 1 μM against PC12 cells comparable to that seen for the best nerve growth factor (NGF) concentration of 40 ng/mL. In addition, evident neuritogenic activity was observed in the cells when treated with gentiside C at a concentration as low as 0.03 μM. The structure–activity relationships within the gentisides A–K revealed that alkyl chain length is important for the activity, but structure diversity at the end of the alkyl chain is not.

1. Introduction

Neurotrophic factors play a critical role in neuronal development, survival, and the functional maintenance of neurons.[1–3] They have been targeted as potential therapeutic drugs for the treatment of neurodegenerative disorders. Nerve growth factor (NGF) is the first and best characterized neurotrophic factor, and is essential for neuronal differentiation, growth, survival, function maintenance, as well as the prevention of aging in the central and peripheral systems.[4–6] Recently, the administration of NGF resulted in the recovery of learning and memory functions in a mouse model of Alzheimer's disease exhibiting NGF deficiency.[7] However, because it is a high-molecular weight polypeptide, NGF is unstable and is also unable to cross the blood–brain barrier.[8] Therefore, its application as a medicine for the treatment of neurodegenerative disorders is assumed to be difficult. To address this issue, considerable efforts have been made to find small molecules that possess neurotrophic properties similar to those of NGF and/or that can enhance the activity of endogenous neurotrophic factors.[9]

The PC12 cell line derived from rat pheochromocytoma cells has been used as an in vitro assay system for screening neuritogenic compounds because it expresses neuronal properties in response to NGF.[10] Our previous research for compounds that mimic and/or enhance the neuritogenic activity of NGF using the PC12 cell line system resulted in the isolation of novel cerebrosides, termitomycesphins from the edible Chinese mushroom *Termitomyces albuminosus*,[11] steroid glycosides named linckosides from the Okinawan blue starfish *Linckia laevigata*,[12] and gentisides from the traditional Chinese medicine *Gentiana rigescens* Franch.[13] Gentisides A (**1**) and B (**2**) having alkyl chains with 22 and 23 carbons, respectively, showed a significant neuritogenic activity at 30 μM against PC12 cells that was comparable to that seen for the best nerve growth factor (NGF) concentration of 40 ng/mL.[13] Further examination of the *G. rigescens* extract has led us to the purification of nine new congeners named gentisides C (**3**), D (**4**), E (**5**), F (**6**), G (**7**), H (**8**), I (**9**), J (**10**), and K (**11**) (Fig. 1). Gentiside C (**3**) possessing the shortest alkyl chain (17 carbons) among all of gentisides showed comparable neuritogenic activity to gentiside A or B at a concentration of 1 μM. This result indicated that gentiside C (**3**) exhibited 30 times stronger activity than that of the reported gentisides. In this paper, we aim to report the isolation, structures, biological activities, and structure–activity relationships of these new neuritogenic compounds.

2. Results and discussion

2.1. Isolation

A methanol extract of the dried roots of *G. rigescens* was partitioned between 80% aqueous MeOH and *n*-hexane. The active *n*-hexane fraction was chromatographed on silica gel, then on

* Corresponding author. Tel./fax: +86 571 88208627.
E-mail address: qijianhua@zju.edu.cn (J. Qi).

0968-0896/$ - see front matter © 2010 Elsevier Ltd. All rights reserved.
doi:10.1016/j.bmc.2010.08.020

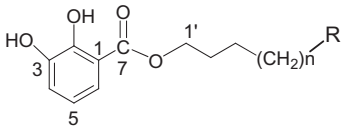

gentiside	R	n	gentiside	R	n
A (**1**)	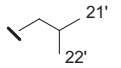	15	F (**6**)	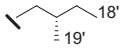	11
B (**2**)	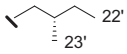	15	G (**7**)	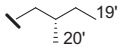	12
C (**3**)	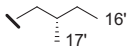	9	H (**8**)	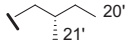	13
D (**4**)	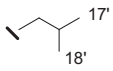	11	I (**9**)		16
E (**5**)		13	J (**10**)		17
			K (**11**)		19

Figure 1. Structures of gentisides A–K (**1**–**11**).

ODS to yield an active fraction. This was further purified by repeated reversed-phase HPLC to yield gentisides C (**3**, 0.00024% of dry wt), D (**4**, 0.00008%), E (**5**, 0.00012%), F (**6**, 0.00015%), G (**7**, 0.00011%), H (**8**, 0.00016%), I (**9**, 0.00005%), J (**10**, 0.00002%), and K (**11**, 0.00002%).

2.2. Structure elucidation

Gentiside C (**3**) was obtained as a colorless powder with the molecular formula $C_{24}H_{40}O_4$ as determined by HR FT-ICR MS measurement. The ^1H and ^{13}C NMR of **3** were superimposable on those of **2** (Tables 1 and 2).[13] The structural difference between **3** and **2** is only the alkyl chain length.[13] Compound **3** possesses six less methene groups than **2** by analysis of HR FT-ICR MS spectra.[13] The absolute stereochemistry of **3** was determined to be the same as that of the **2** by comparison of their optical rotation [**2**: $[\alpha]_D^{22}$ +2.4 (*c* 2.0, $CHCl_3$); **3**: $[\alpha]_D^{22}$ +2.9 (*c* 0.5, $CHCl_3$)].[13] Therefore, the structure of **3** was determined as shown in Figure 1.

Gentiside D (**4**) was obtained as a colorless powder with the molecular formula $C_{25}H_{42}O_4$ as determined by HR FT-ICR MS measurement. The ^1H and ^{13}C NMR of **4** were superimposable on those of **1** (Tables 1 and 2).[13] The only structural difference between **4** and **1** is the alkyl chain length. Compound **4** possesses four less methene groups than **1** by analysis of HR FT-ICR MS spectra. Therefore, the structure of **4** was determined as shown in Figure 1.

Gentiside E (**5**) was obtained as a colorless powder with the molecular formula $C_{25}H_{42}O_4$ as determined by HR FT-ICR MS measurement. The IR absorption band at 3470 cm^{-1} suggested the presence of a hydroxyl group. The proton nuclear magnetic resonance (^1H NMR) spectrum indicated the presence of one methyl (CH_3) group (δ_H 0.88), many aliphatic methylene (CH_2) and/or methine (CH) groups (δ_H 1.21–1.77), a benzene ring (δ_H 6.80–7.37), one oxygen functionality (CH_n–O, δ_H 4.34), and two singlet hydroxyl groups (δ_H 5.64 and 11.01). One only tripleted methyl signal (δ_H 0.88, *J* = 7.0 Hz) revealed the presence of a linear chain at the end of the long alkyl chain. The sharp signal of a hydroxyl group at δ_H 11.01 is due to the formation of a hydrogen bond with a carboxyl group. The signals at δ_H 0.88 (t) and many aliphatic methylenes δ_H 1.21–1.77, δ_C 22.7–31.9 suggested the presence of a long alkyl with a linear chain at the end of alkyl chain in this molecule. The signal at δ_C 170.4 supported the presence of one carboxyl group. The ^{13}C and DEPT NMR data combined with 2D NMR, as well as HR-MS data, confirmed the presence of one CH_3, 16 CH_2, one CH_2–O, one benzene ring with three substituted positions, and one carboxyl group. Taking the molecular formula into consideration, two of the three substituted positions of the benzene ring turned out to be two hydroxyl groups. The analysis of COSY and HOHAHA spectra led to the determination of partial structures (C-4 to C-6, C-1′ to C-3′, and a long alkyl chain) depicted by the bold bonds in Figure 2. These partial structures were connected by the long-range H–C correlations obtained by an HMBC experiment to give a gross structure of **5**. The HMBC correlations establishing the gross structure of **5** were as follows: a proton of the hydroxyl group at C-2 to C-1, C-2, and C-3; a proton of the hydroxyl group at C-3 to C-2, C-3, and C-4; H-6 to C-7; H-1′ to C-7. The important HMBC correlations are summarized in Figure 2 with arrows. Thus, the structure of **5** was elucidated as shown in Figure 1.

Gentiside F (**6**) was obtained as a colorless powder with the molecular formula $C_{26}H_{44}O_4$ as determined by HR FT-ICR MS measurement. The ^1H and ^{13}C NMR of **6** were superimposable on those of **2** (Tables 1 and 2).[13] The only structural difference between **6** and **2** is the alkyl chain length.[13] Compound **6** possesses four less methene groups than **2** by analysis of HR FT-ICR MS spectra.[13] The absolute stereochemistry of **6** was determined to be the same as that of **2** by comparison of their optical rotation [**2**: $[\alpha]_D^{22}$ +2.4 (*c* 2.0, $CHCl_3$); **6**: $[\alpha]_D^{22}$ +3.0 (*c* 0.1, $CHCl_3$)].[13] Therefore, the structure of **6** was determined as shown in Figure 1.

Gentiside G (**7**) was obtained as a colorless powder with the molecular formula $C_{27}H_{46}O_4$ as determined by HR FT-ICR MS

Table 1
^{1}H NMR data for gentisides C–K (**3**–**11**)[a] ($CDCl_3$)

Carbon No.	3	4	5	6	7	8	9	10	11
1	—	—	—	—	—	—	—	—	—
2	—	—	—	—	—	—	—	—	—
3	—	—	—	—	—	—	—	—	—
4	7.10 dd (8.0, 1.0)	7.10 dd (7.5, 1.0)	7.10 dd (8.0, 1.5)	7.10 dd (7.0, 1.0)	7.10 dd (7.0, 1.5)	7.10 dd (8.0, 1.0)	7.10 dd (8.0, 1.5)	7.10 dd (8.0, 1.5)	7.10 dd (8.0, 1.5)
5	6.80 t (8.0)	6.80 t (8.0)	6.80 t (7.5)	6.80 t (8.0)	6.80 t (7.5)	6.80 t (8.0)	6.80 t (8.0)	6.80 t (8.0)	6.80 t (8.0)
6	7.37 dd (8.0, 1.0)	7.37 dd (7.0, 1.0)	7.37 dd (8.0, 1.5)	7.37 dd (7.0, 1.0)	7.37 dd (8.0, 1.5)	7.37 dd (8.0, 1.0)	7.37 dd (8.0, 1.5)	7.37 dd (8.0, 1.5)	7.37 dd (8.0, 1.5)
7	—	—	—	—	—	—	—	—	—
1′	4.34 t (6.5)	4.34 t (6.5)	4.34 t (6.5)	4.34 t (6.5)	4.34 t (6.5)	4.34 t (6.5)	4.34 t (6.5)	4.34 t (6.5)	4.34 t (6.5)
2′	1.78 m	1.77 m	1.77 m	1.77 m	1.77 m	1.77 m	1.77 m	1.77 m	1.77 m
3′	1.44 m	1.43 m	1.43 m	1.43 m	1.43 m	1.43 m	1.42 m	1.45 m	1.43 m
4′-13′	1.09–1.38 m	1.23–1.38 m	1.21–1.38 m	1.09–1.36 m	1.08–1.36 m	1.08–1.36 m	1.21–1.37 m	1.22–1.39 m	1.21–1.37 m
14′	1.34 m	1.23–1.38 m	1.21–1.38 m	1.09–1.36 m	1.08–1.36 m	1.08–1.36 m	1.21–1.37 m	1.22–1.39 m	1.21–1.37 m
15′	1.10, 1.30 m	1.15 m	1.21–1.38 m	1.09–1.36 m	1.08–1.36 m	1.08–1.36 m	1.21–1.37 m	1.22–1.39 m	1.21–1.37 m
16′	0.85 t (7.0)	1.51 m	1.21–1.38 m	1.35 m	1.08–1.36 m	1.08–1.36 m	1.21–1.37 m	1.22–1.39 m	1.21–1.37 m
17′	0.84 d (6.0)	0.86 d (6.5)	1.21–1.38 m	1.10, 1.30 m	1.35 m	1.08–1.36 m	1.21–1.37 m	1.22–1.39 m	1.21–1.37 m
18′	—	0.86 d (6.5)	0.88 t (7.0)	0.86 t (7.5)	1.10, 1.30 m	1.35 m	1.21–1.37 m	1.22–1.39 m	1.21–1.37 m
19′	—	—	—	0.84 d (6.5)	0.85 t (6.5)	1.10, 1.30 m	1.21–1.37 m	1.22–1.39 m	1.21–1.37 m
20′	—	—	—	—	0.84 d (6.0)	0.85 t (7.5)	1.21–1.37 m	1.22–1.39 m	1.21–1.37 m
21′	—	—	—	—	—	0.84 d (6.5)	0.88 t (6.5)	1.22–1.39 m	1.21–1.37 m
22′	—	—	—	—	—	—	—	0.88 t (6.5)	1.21–1.37 m
23′	—	—	—	—	—	—	—	—	1.21–1.37 m
24′	—	—	—	—	—	—	—	—	0.88 t (6.5)
2-OH	11.00 s	11.00 s	11.01 s	11.00 s	11.01 s	11.00 s	11.00 s	11.00 s	11.00 s
3-OH	5.64 s	5.63 s	5.64 s	5.63 s	5.64 s	5.63 s	5.63 s	5.62 s	5.63 s

[a] 500 MHz, coupling constants (*J* in Hz) are in parentheses.

Table 2
^{13}C NMR data for gentisides C–I (**3**–**9**)[a] ($CDCl_3$)

Carbon No.	3	4	5	6	7	8	9
1	112.7	112.7	112.7	112.7	112.7	112.7	112.7
2	148.9	148.9	148.9	148.9	148.9	148.9	148.9
3	145.0	145.0	145.0	145.0	145.0	145.0	145.0
4	119.7	119.7	119.6	119.6	119.6	119.7	119.6
5	119.1	119.1	119.1	119.1	119.1	119.1	119.1
6	120.5	120.5	120.5	120.5	120.5	120.5	120.5
7	170.4	170.4	170.4	170.4	170.4	170.4	170.1
1′	65.7	65.7	65.7	65.7	65.7	65.7	65.7
2′	28.5	28.5	28.5	28.5	28.5	28.5	28.5
3′	25.9	25.9	25.9	25.9	25.9	26.0	25.9
4′-13′	27.1–30.0[b]	27.4–29.9[c]	29.2–29.7[d]	27.1–30.0[b]	27.1–30.0[b]	27.1–30.0[b]	29.2–29.7[d]
14′	34.4	27.4–29.9[c]	29.2–29.7[d]	27.1–30.0[b]	27.1–30.0[b]	27.1–30.0[b]	29.2–29.7[d]
15′	36.7	39.1	29.2–29.7[d]	27.1–30.0[b]	27.1–30.0[b]	27.1–30.0[b]	29.2–29.7[d]
16′	11.4	28.0	31.9	34.4	27.1–30.0[b]	27.1–30.0[b]	29.2–29.7[d]
17′	19.2	22.6	22.7	36.6	34.3	27.1–30.0[b]	29.2–29.7[d]
18′		22.6	14.1	11.4	36.6	34.4	29.2–29.7[d]
19′				19.2	11.4	36.6	31.9
20′					19.2	11.4	22.7
21′						19.3	14.1

[a] 125 MHz.
[b] δ: 27.1, 29.2, 29.5, 29.6, 29.7, 30.0.
[c] δ: 27.4, 29.2, 29.5, 29.6, 29.7, 29.9.
[d] δ: 29.2, 29.4, 29.5, 29.6, 29.7.

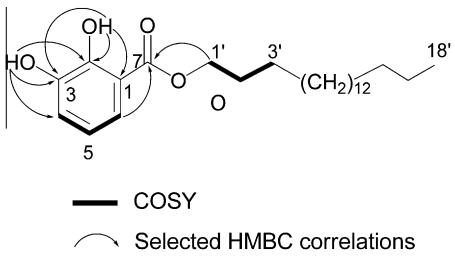

Figure 2. Gross structure of gentiside E (**5**) with selected HMBC correlations.

measurement. The ^{1}H and ^{13}C NMR of **7** were superimposable on those of **2** (Tables 1 and 2).[13] The only structural difference between **7** and **2** is the alkyl chain length.[13] Compound **7** possesses three less methene groups than **2** by analysis of HR FT-ICR MS spectra.[13] The absolute stereochemistry of **7** was determined to be the same as that of **2** by comparison of their optical rotation [**2**: $[\alpha]_D^{22}$ +2.4 (*c* 2.0, $CHCl_3$); **7**: $[\alpha]_D^{22}$ +3.1 (*c* 0.1, $CHCl_3$)].[13] Therefore, the structure of **7** was determined as shown in Figure 1.

Gentiside H (**8**) was obtained as a colorless powder with the molecular formula $C_{28}H_{48}O_4$ as determined by HR FT-ICR MS measurement. The ^{1}H and ^{13}C NMR of **8** were superimposable on those of **2** (Tables 1 and 2).[13] The only structural difference between **8** and **2** is the alkyl chain length.[13] Compound **8** possesses two less methene groups than **2** by analysis of HR FT-ICR MS spectra.[13] The absolute stereochemistry of **8** was determined to be the same as that of **2** by comparison of their optical rotation [**2**: $[\alpha]_D^{22}$ +2.4

(c 2.0, $CHCl_3$); **8**: $[\alpha]_D^{22}$ +2.3 (c 2.0, $CHCl_3$)].[13] Thus, the structure of **8** was determined as shown in Figure 1.

Gentiside I (**9**) was obtained as a colorless powder with the molecular formula $C_{28}H_{48}O_4$ as determined by HR FT-ICR MS measurement. The ^1H and ^{13}C NMR of **9** were superimposable on those of **5** (Tables 1 and 2). The only structural difference between **9** and **5** is the alkyl chain length. Compound **9** possesses three more methene groups than **5** by analysis of HR FT-ICR MS spectra. Thus, the structure of **9** was determined as shown in Figure 1.

Gentiside J (**10**) was obtained as a colorless powder with the molecular formula $C_{29}H_{50}O_4$ as determined by HR FT-ICR MS measurement. Due to a small amount of gentiside J (**10**) in hand, the ^{13}C NMR was not measured. The ^1H NMR of **10** was superimposable on that of **5** (Table 1). The only structural difference between **10** and **5** is the alkyl chain length. Compound **10** possesses four more methene groups than **5** by analysis of HR FT-ICR MS spectra. Thus, the structure of **10** was determined as shown in Figure 1.

Gentiside K (**11**) was obtained as a colorless powder with the molecular formula $C_{31}H_{54}O_4$ as determined by HR FT-ICR MS measurement. Due to a small amount of gentiside K (**11**) obtained, the ^{13}C NMR was not measured. The ^1H NMR of **11** was superimposable on that of **5** (Table 1). The only structural difference between **11** and **5** is the alkyl chain length. Compound **11** possesses six more methene groups than **5** by analysis of HR FT-ICR MS spectra. Therefore, the structure of **11** was determined as shown in Figure 1.

2.3. Biological activity

The neuritogenic activity of gentisides C–K (**3–11**) was evaluated using PC12 cells and compared to the activity of 40 ng/mL NGF. Gentiside C (**3**) exhibited the best neuritogenic activity among all gentisides. It showed a dose-dependent increasing activity ranging from 0.03 to 1 μM as shown in Figure 3. At the best concentration (1 μM) without obvious cytotoxicity, gentiside C exhibited neurite outgrowth equivalent to that seen with the positive NGF control at its best concentration (40 ng/mL). Even at a concentration as low as 0.03 μM, gentiside C showed significant neuritogenic activity against PC12 cells. The solvent control also induced few neurite outgrowths.

Figure 4 shows the morphological changes in the PC12 cells after treatment with gentiside C (**3**, Fig. 4c and d) compared with the solvent control (0.5% DMSO, Fig. 4a) and the positive NGF control (40 ng/mL, Fig. 4b). When treated with gentiside C (**3**) at 1 μM (Fig. 4d), the cells had long multipolar and bipolar neurite outgrowths 48 h after treatment, which were similar to those produced following treatment with NGF at 40 ng/mL. Obvious neurite outgrowths were observed when treated with gentiside C (**3**) at a low concentration of 0.03 μM (Fig. 4c). Control cells cultured without additional compounds induced few short neurite outgrowths.

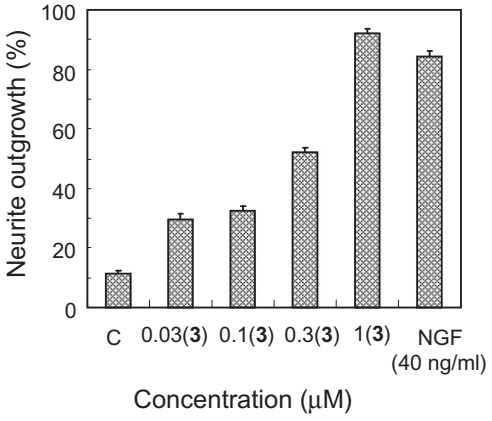

Figure 3. Dose-dependent response of the NGF-mimicking activity of gentiside C (**3**) 48 h after treatment. C: control (0.5% DMSO); NGF (40 ng/mL): positive control.

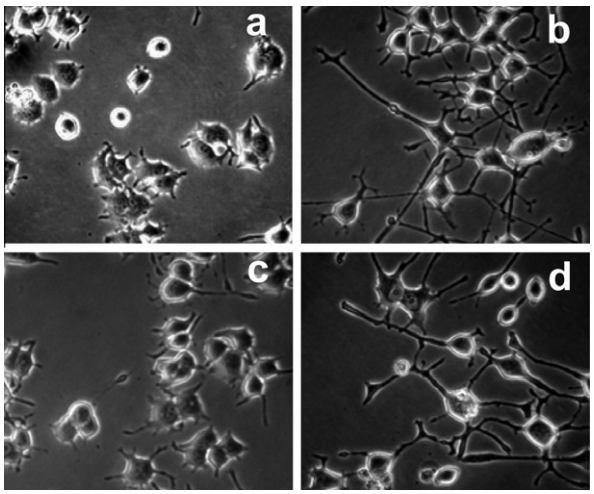

Figure 4. Photomicrographs of PC12 cells under a phase-contrast microscope 48 h after treatment: (a) solvent control (0.5% DMSO), (b) NGF (40 ng/mL), (c) gentiside C (**3**, 0.03 μM), and (d) gentiside C (**3**, 1 μM).

Figure 5 shows the maximum activity of gentisides C–K (**3–11**) in the percentage of PC12 cells with long neurite outgrowths. The maximum activity of each gentiside was observed at the best concentration without cytotoxicity 48 h after treatment. Gentisides C–J (**3–10**) exhibited maximum neuritogenic activities of 67–91%, and the concentrations varied from 1 to 30 μM, which corresponded to the best concentration for the maximum activity of each gentiside. While gentiside K (**11**) showed maximum neuritogenic activities of 48% at 30 μM. The poor solubility of **11** affected its biological activity. The gentisides had varying alkyl chain lengths, with or without an isobutyl or isopropyl group at the end of the alkyl chain. The structure–activity relationship among gentisides revealed that alkyl chain length plays an important role in the neuritogenic activity of gentisides. However, structure diversity at the end of the alkyl chain did not have obvious affects on the activity. Gentiside C (**3**) possesses the shortest alkyl chain length of 17 carbons and exhibited the best activity, inducing 91% neuritogenic activities at a concentration of 1 μM. However, gentiside K (**11**) which has the longest alkyl chain length of 24 carbons stimulated neuritogenic activities of 48% at 30 μM, in which the concentration was 30 times higher than that of the gentiside C (**3**) (Fig. 5).

3. Experimental

3.1. General procedures

Preparative HPLC was performed using ELITE P-230 pumps. IR spectra were measured on a JASCO FT/IR-4100 and the UV spectra were recorded on a PGENERAL TU-1901. The optical rotations were recorded on a JASCO P-1030 digital polarimeter. High-resolution (HR) MS measurements were performed on a Apex III (7.0 Tesla) FTICR mass spectrometer (Bruker, Billerica, MA, USA) using CF_3COONa as an external calibration standard. The NMR spectra were measured on a Bruker AV III-500 spectrometer, and the NMR chemical shifts in δ (ppm) were referenced to the solvent peaks of δ_H 7.26 and δ_C 77.0 for $CDCl_3$.

3.2. Extraction and isolation

The extraction and purification procedures were described in detail in a previous paper.[13] The n-hexane fraction from the MeOH extract of the dried roots of *G. rigescens* was chromatographed on

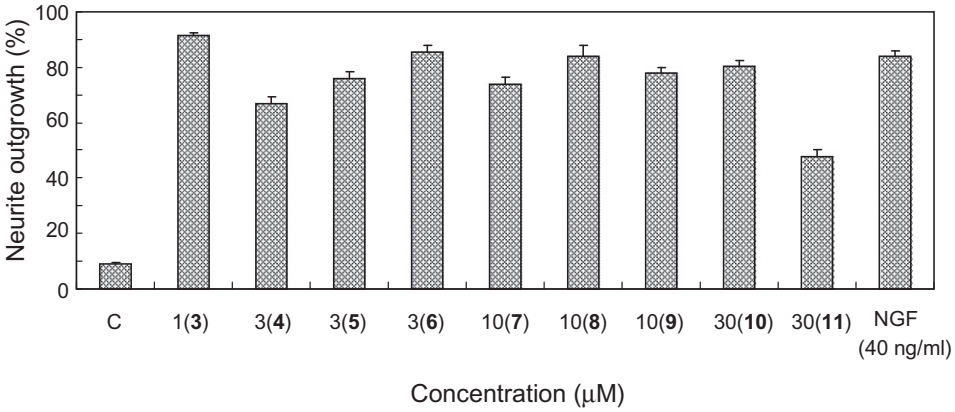

Figure 5. Maximum NGF-mimicking activity of gentisides C–K (**3**–**11**) at the best concentration. C: control (0.5% DMSO); NGF (40 ng/mL): positive control.

silica gel to give an active fraction which was separated through ODS to afford an active fraction. The active sample was subjected to HPLC [10 times, Develosil ODS-HG-5 (φ 10/250 mm), Nomura chemical, flow rate: 3 mL/min, MeOH/H_2O (98:2)] to give 11 active fractions. Gentisides A (**1**) and B (**2**) were obtained from two of these fractions.[13] The remaining nine active samples were purified by HPLC [Develosil ODS-HG-5 (φ 10/250 mm), Nomura chemical, flow rate: 3 mL/min] in sequence according to the retention time using similar purification conditions. The first active fraction with the shortest retention time was first purified (85–100% aqueous EtOH in 60 min linear gradient) to give pure gentiside C (**3**) (4.8 mg, t_R = 26.1 min). Using the same or similar HPLC purification condition as that of gentiside C, gentiside D (**4**) (1.6 mg, t_R = 29.2 min, 85–100% aqueous EtOH in 60 min linear gradient), gentiside E (**5**) (2.3 mg, t_R = 37.3 min, 85–100% aqueous EtOH in 120 min linear gradient), gentiside F (**6**) (2.9 mg, t_R = 32.2 min, 85–100% aqueous EtOH in 60 min linear gradient), gentiside G (**7**) (2.2 mg, t_R = 43.0 min, 85–100% aqueous EtOH in 90 min linear gradient), gentiside H (**8**) (3.2 mg, t_R = 44.7 min, 85–100% aqueous EtOH in 90 min linear gradient), gentiside I (**9**) (1.0 mg, t_R = 47.0 min, 85–100% aqueous EtOH in 90 min linear gradient), gentiside J (**10**) (0.4 mg, t_R = 36.1 min, 90–100% aqueous EtOH in 60 min linear gradient), and gentiside K (**11**) (0.4 mg, t_R = 36.9 min, 90–100% aqueous EtOH in 60 min linear gradient) were obtained.

3.2.1. Gentiside C (3)

Colorless powder, $[\alpha]_D^{22}$ +2.9 (*c* 0.5, $CHCl_3$), IR (KBr): 3457, 2925, 1675, 1469, 1303, 1119, 1066 cm^{-1}; UV (MeCN) λ_{max} (log ε): 318 nm (4.6); HR FT-ICR MS *m*/*z* 391.2844 $(M-H)^-$, calcd for $C_{24}H_{39}O_4$ 391.2854; for ^1H and ^{13}C NMR see Tables 1 and 2.

3.2.2. Gentiside D (4)

Colorless powder, IR (KBr): 3446, 2923, 1674, 1463, 1303, 1120, 1070 cm^{-1}; UV (MeCN) λ_{max} (log ε): 321 nm (4.7); HR FT-ICR MS *m*/*z* 405.2999 $(M-H)^-$, calcd for $C_{25}H_{41}O_4$ 405.3010; for ^1H and ^{13}C NMR see Tables 1 and 2.

3.2.3. Gentiside E (5)

Colorless powder, IR (KBr): 3470, 2919, 1668, 1468, 1300, 1149, 1068 cm^{-1}; UV (MeCN) λ_{max} (log ε): 317 nm (4.8); HR FT-ICR MS *m*/*z* 405.2997 $(M-H)^-$, calcd for $C_{25}H_{41}O_4$ 405.3010; for ^1H and ^{13}C NMR see Tables 1 and 2.

3.2.4. Gentiside F (6)

Colorless powder, $[\alpha]_D^{22}$ +3.0 (*c* 0.1, $CHCl_3$); IR (KBr): 3442, 2925, 1671, 1469, 1309, 1154, 1071 cm^{-1}; UV (MeCN) λ_{max} (log ε): 318 nm (5.9); HR FT-ICR MS *m*/*z* 419.3154 $(M-H)^-$, calcd for $C_{26}H_{43}O_4$ 419.3167; for ^1H and ^{13}C NMR see Tables 1 and 2.

3.2.5. Gentiside G (7)

Colorless powder, $[\alpha]_D^{22}$ +3.1 (*c* 0.1, $CHCl_3$); IR (KBr): 3478, 2920, 1671, 1463, 1326, 1147, 1071 cm^{-1}; UV (MeCN) λ_{max} (log ε): 321 nm (4.9); HR FT-ICR MS *m*/*z* 433.3310 $(M-H)^-$, calcd for $C_{27}H_{45}O_4$ 433.3323; for ^1H and ^{13}C NMR see Tables 1 and 2.

3.2.6. Gentiside H (8)

Colorless powder, $[\alpha]_D^{22}$ +2.3 (*c* 2.0, $CHCl_3$); IR (KBr): 3458, 2918, 1650, 1440, 1301, 1150, 1064 cm^{-1}; UV (MeCN) λ_{max} (log ε): 318 nm (4.8); HR FT-ICR MS *m*/*z* 447.3463 $(M-H)^-$, calcd for $C_{28}H_{47}O_4$ 447.3480; for ^1H and ^{13}C NMR see Tables 1 and 2.

3.2.7. Gentiside I (9)

Colorless powder; IR (KBr): 3478, 2925, 1675, 1469, 1309, 1154, 1071 cm^{-1}; UV (MeCN) λ_{max} (log ε): 318 nm (4.1); HR FT-ICR MS *m*/*z* 447.3464 $(M-H)^-$, calcd for $C_{28}H_{47}O_4$ 447.3480; for ^1H and ^{13}C NMR see Tables 1 and 2.

3.2.8. Gentiside J (10)

Colorless powder; HR FT-ICR MS *m*/*z* 461.3627 $(M-H)^-$, calcd for $C_{29}H_{49}O_4$ 461.3636; for ^1H NMR see Table 1.

3.2.9. Gentiside K (11)

Colorless powder; HR FT-ICR MS *m*/*z* 489.3931 $(M-H)^-$, calcd for $C_{31}H_{53}O_4$ 489.3949; for ^1H NMR see Table 1.

3.3. Bioassay methods

Biological activity was evaluated according to the methods described in our previous papers.[11,12] Briefly, 20,000 of PC12 cells in DMEM medium were placed in each well (1 mL medium) of a 24-well microplate and precultured under a humidified atmosphere of 5% CO_2 at 37 °C. The medium was replaced by 1 mL of serum-free DMEM medium containing a test sample and DMSO (0.5%) 24 h later. The morphological changes of the cells were monitored under a phase-contrast microscope at every 24 h. About one hundred cells were counted from a randomly chosen field and this was repeated three times. Activity is represented by percentages of PC12 cells with neurite outgrowths longer than the diameter of the cell body.

Acknowledgments

This work was financially supported by NSFC (30873152) and Science Foundation of Chinese University (2009QNA7023).

References and notes

1. Berninger, B.; Poo, M. M. *Nature* **1999**, *401*, 862.
2. Kromer, L. F. *Science* **1987**, *235*, 214.
3. Thoenen, H. *Science* **1995**, *270*, 593.
4. Hefti, F.; Weiner, W. J. *Ann. Neurol.* **1986**, *20*, 275.
5. Hefti, F.; Hartikka, J.; Knusel, B. *Neurobiol. Aging* **1989**, *10*, 515.
6. Barde, Y. A. *Neuron* **1989**, *2*, 1525.
7. Rosa, R. D.; Garcia, A. A.; Braschi, C.; Capsoni, S.; Maffei, L.; Berardi, N.; Cattaneo, A. *Proc. Natl. Acad. Sci. U.S.A.* **2005**, *102*, 3811.
8. Granholm, A. C.; Albeck, D.; Backman, C.; Curtis, M.; Ebendal, T.; Friden, P.; Henry, M.; Hoffer, B.; Kordower, J.; Rose, G. M.; Soderstrom, S.; Bartus, R. T. *Rev. Neurosci.* **1998**, *9*, 31.
9. Brinton, R. D.; Yamazaki, R. S. *Pharm. Res.* **1998**, *15*, 386.
10. Greene, L. A.; Tischler, A. S. *Proc. Natl. Acad. Sci. U.S.A.* **1976**, *73*, 2424.
11. Qi, J.; Ojika, M.; Sakagami, Y. *Tetrahedron* **2000**, *56*, 5835.
12. Qi, J.; Ojika, M.; Sakagami, Y. *Bioorg. Med. Chem.* **2002**, *10*, 1961.
13. Gao, L.; Li, J.; Qi, J. *Bioorg. Med. Chem.* **2010**, *18*, 2131.